Am J Cancer Res 2025;15(4):1647-1661
www.ajcr.us /ISSN:2156-6976/ajcr0162240

Original Article

Disulfiram potentiates cisplatin-induced apoptosis in small cell lung cancer via the inhibition of cystathionine β-synthase and H_2S

Yongguang Wang[1,2*], Ruiping Du[2,3*], Rong Gao[1,2*], Chang Guo[1,2], Jian Qi[2,3], Yani Zhang[2,3], Qizhi Zhu[3], Qingmei Deng[2], Zongtao Hu[2], Hongzhi Wang[1,2,3], Bo Hong[1,2,3]

[1]School of Basic Medical Sciences, Anhui Medical University, Hefei 230032, Anhui, China; [2]Hefei Cancer Hospital of CAS, Institute of Health and Medical Technology, Hefei Institutes of Physical Science, Chinese Academy of Sciences (CAS), Hefei 230031, Anhui, China; [3]University of Science and Technology of China, Hefei 230026, Anhui, China. [*]Co-first authors.

Received November 25, 2024; Accepted April 3, 2025; Epub April 15, 2025; Published April 30, 2025

Abstract: Small cell lung cancer (SCLC) is a highly malignant neuroendocrine tumor. Platinum-based chemo-resistance is the major issue for the treatment of SCLC. The objective of the study is to identify the drugs that enhance anti-tumor activity of cisplatin (CDDP) in SCLC. Firstly, by a high-throughput drug screening, we found that disulfiram (DSF), a FDA-approved drug that is used to treat alcohol addiction, was able to sensitize CDDP-induced apoptosis in SCLC. RNA-seq analysis revealed that cystathionine β-synthase (CBS) was a potential target of combination treatment of DSF and CDDP in SCLC. CDDP treatment induced CBS expression, while the elevation of CBS expression was down-regulated by DSF and CDDP co-treatment in SCLC. Importantly, the down-regulation of CBS by siRNA silence increased CDDP-induced cellular apoptosis in SCLC. Furthermore, the study found that DSF combined with CDDP decreased the H_2S level, and increased the level of ROS. The elevation of H_2S level reduced the growth inhibition of SCLC cells by DSF and CDDP co-treatment. Finally, in nude mice bearing SCLC xenografts, DSF and CDDP co-treatment exhibited remarkable anti-tumor activity against SCLC tumors, evidenced by the significant reduction of tumor size, tumor weight and Ki-67 expression as compared with single treatment alone. Therefore, the study indicated that DSF could be re-purposed to potentiate CDDP-induced anti-tumor activity in SCLC, which are worth immediate assessment for SCLC in clinical settings.

Keywords: Small cell lung cancer, chemo-resistance, cisplatin, disulfiram, cystathionine β-synthase, H_2S

Introduction

Lung cancer can be divided into non-small cell lung cancer (NSCLC) and small cell lung cancer (SCLC) in histological subtypes [1]. SCLC, accounting for 15% of all lung cancer cases, has the worst prognosis. The overall 5-year survival rate for SCLC is only 5%, making it the sixth leading cause of cancer-related death [2]. SCLC has the characteristics of high proliferation rate and early metastasis [3]. Genomic analyses indicated that SCLC had high mutation burden and extensive chromosome rearrangements, almost always involving *TP53* and *RB1* mutations, and often accompanied by *MYC* oncogene amplification [4, 5]. SCLC patients responded to initial platinum-based chemo-therapy, but they almost developed chemo-resistance quickly within 6 months [6]. Therefore, chemotherapy resistance is an urgent issue in clinic to improve the survival of SCLC patients.

To identify the drugs that are able to enhance the sensitivity of cisplatin (CDDP) in SCLC, our previous study carried out a high throughput drug screening. By screening 1092 FDA-approved drugs, we found that auranofin, a drug for the treatment of rheumatoid arthritis, sensitized SCLC cells to CDDP treatment [7]. In the meanwhile, the screening also found that disulfiram (DSF) increased the inhibitory effect of CDDP on SCLC cells' growth. DSF is a FDA-approved drug that is used to treat the alcohol

addiction in the clinic, but an increasing number of studies have indicated that DSF has anti-tumor effect in different kind of cancer types, such as NSCLC, liver cancer, breast cancer and so on [8]. Previous study has showed that DSF inhibited ALDH activity to target cancer stem cells to overcome chemotherapy resistance in breast cancer [9]. DSF inhibited the activity of NF-κB signaling pathway and enhanced 5-Fu induced-apoptosis of colon cancer cells [10]. DSF significantly increased the sensitivity of pancreatic cancer cells and xenografted nude mice to ionizing radiation by aggravating DNA damage, inducing cell cycle arrest and apoptosis [11]. In BCR-ABL+ leukemia cells, DSF synergized with tyrosine kinase inhibitors by inducing ferroptosis via promoting GPX4 degradation [12]. DSF can also enhance the efficacy of anti-immune checkpoints therapy. In triple-negative breast cancer, DSF reduced the methylation in the IRF7 promoter through DNMT1, thus increasing the expression of PD-L1 and enhancing anti-tumor efficacy of anti-PD-1 antibody [13]. DSF inhibited the malignant progression of esophageal squamous cell carcinoma by blocking MOF deubiquitination controlled by USP21 [14]. Wang et al. have demonstrated that DSF activated T-cell antigen receptor signaling to induce anti-tumor response of $CD8^+$ T cells [15]. Terashima et al. have indicated that DSF also reduced the aggregation of macrophages in the tumor by preventing chemokine FROUNT from interacting with its receptor, thereby inhibiting tumor growth and metastasis [16]. The anti-tumor activity of DSF is thought to be copper ions dependent [17-20]. DSF is metabolized as diethyldithiocarbamate (DTC) in the body and can form a complex with copper ions, CuET, which exerts an anti-cancer effect [21]. In SCLC, the synergistic anti-tumor activity of DSF with CDDP has not been reported so far.

In the study, we found that DSF enhanced the anti-tumor activity of CDDP *in vitro* and *in vivo* in SCLC. RNA-seq analysis identified cystathionine β-synthase (CBS), which was a potential target for DSF-CDDP combination treatment. The synergistic action of DSF and CDDP was through H_2S reduction and ROS overproduction. Our study suggests that DSF is a promising chemo-sensitizer of CDDP-based therapy in SCLC.

Materials and methods

Cell lines

Human SCLC cell lines, H69, H446, H82, H196 and H526 were cultured in RPMI-1640 complete medium (Corning, Cellgro, Manassas, VA, USA) in a humidified incubator at 37°C in 5% CO_2.

Materials

CDDP was obtained from Selleck chemical (Shanghai, China) and dissolved in PBS at a stock concentration of 1 mM. DSF was from MCE chemical (Shanghai, China) and dissolved in DMSO (Sigma-Aldrich, Saint Louis, MO, USA) at a stock concentration of 10 mM. PARP (9542S, 1:1000 dilution) and CBS (14782S, 1:1000 dilution) antibodies were purchased from Cell Signaling Technology (Danvers, MA, USA). β-actin (HC201-02, 1:10000 dilution) antibody was obtained from TransBionovo (Beijing, China).

Cell viability assay

The CellTiter-Glo Luminescent assay (Promega, Madison, WI, USA) was used to detect cell viability. 3000 cells/well were seeded in 96-well plate (Coring Costar, ME, USA). After 24 hr, the cells were subjected to the treatment of control or the drugs for 72 hr in triplicate. Then, an equal volume of CellTiter-Glo reagent was added and incubated at room temperature for 10 min. Luminescent signal was measured in a multilabel plate reader (Molecular Devices, CA, USA).

High-throughput drug screen

A JANUS automated liquid handling workstation (PerkinElmer, Waltham, MA, USA) was used to screen FDA-approved drugs that enhanced the anti-tumor activity of CDDP as previously described [7].

Cell apoptosis

After control or drug treatment, SCLC cells were stained with FITC Annexin V and PI using an Apoptosis Detection Kit (BD Pharmingen, San Diego, CA, USA), and then analyzed on flow cytometry (CytExpert, Beckman Coulter, Brea, CA, USA). The results were analyzed using

FlowJo software (BD Pharmingen, Ashland, OR, USA).

Western blot

After treatment, SCLC cells were lysed with protein lysis buffer (150 mM NaCl, 50 mM Tris-HCl (pH 8.0), 1% Triton X-100, 2 mM EDTA, 1× Proteinase Inhibitor), and then protein lysate was quantified using BCA Assay Kit (Beyotime, Shanghai, China). 20 μg protein was subjected to SDS-polyacrylamide gel (10%) electrophoresis, and then transferred to PVDF membrane (Merck Millipore, Germany). The PVDF membrane was blocked with 5% milk for 2 hr, and then incubated with a primary antibody at 4°C overnight, and followed by incubation with a secondary antibody for 2 hr at room temperature. Signals were detected by an ECL substrate (Zen-bioscience, Cheng Du, China). The band density was quantified by ImageJ (NIH, USA). β-actin was used as a loading control for normalization.

RNA-seq

H69 cells was treated with DMSO control, 2 μM CDDP, 0.025 μM DSF and CDDP combined with DSF for 24 hr, and total RNA was extracted using RNA Easy Fast Tissue/cell Kit (Tiangen, Beijing, China). mRNA was enriched using the VAHTS mRNA Capture Beads (Vazyme, Jiangsu, China). Libraries were prepared with the VAHTS Universal V8 RNA-Seq Library Prep Kit (Vazyme, Jiangsu, China), and then paired-end sequenced on Illumina NovaSeq 6000 machines (Illumina, CA, USA) to generate 150 bp paired-end reads. Raw reads were trimmed using Trim Galore (v0.6.7) to remove the low-quality reads. The clean reads were then aligned to the GRCh37 genome using STAR (v2.7.10b), and quantification was performed with RSEM (v1.3.1). Normalization and differential expression analysis were conducted using R package edgeR with gene count matrices. Log fold change (FC) >1 and false discovery rate (FDR) <0.05 were considered to be differentially expressed genes.

siRNA and transfection

H446 cells at 70% to 80% confluence were transfected with siRNA following the instructions provided by the Lipofectamine 2000 kit (Invitrogen, MA, USA). siRNA sequence is listed as below: CBS siRNA: 5'-CAGACCAAGUUGGCAAAGUTT-3'. Control siRNA: 5'-UUCUCCGAACGUGUCACGUTT-3'.

Measurement of ROS generation

H446 cells were plated in 6-well plates at a density of 5×10^5 cells/well. After 24 hr, cells were treated by vehicle control and drugs for 4 hr. And then DCFH-DA probe (Beyotime Biotech, Shanghai, China) was added to the 6-well plate and incubated with the cells for 30 min, away from light. After washed twice with PBS, the fluorescence of ROS was observed by fluorescence microscope (Carl Zeiss AG, Germany).

Detection of intracellular H_2S level

We used a fluorescent probe WSP-5 (Cayman Chemical, Michigan, USA) to detect H_2S level in SCLC cells, according to the method of Peng et al. [22]. Briefly, after H446 cells were treated with DMSO or drugs for 4 hr, WSP-5 (50 μM) and a surfactant hexadecyltrimethylammonium bromide (CTAB, 100 μM) in serum-free medium were added to cells, and then incubated at 37°C for 20 min in the dark. After washed with PBS twice, fluorescence signal was observed under a fluorescent microscope (Carl Zeiss AG, Germany).

Xenograft experiments

5-week-old female nude mice (Vital River Laboratory Animal Technology, Beijing, China) were inoculated subcutaneously with H69 cells (2×10^6/100 μl medium) mixed with 100 μl of Matrigel (BD Biosciences, Franklin, NJ, USA) in the inguinal region of both hind limbs. Mice were raised in specific pathogen free (SPF)-grade animal house (22°C, 50% Relative Humidity). When tumors grew to 4-5 mm in diameter, mice were randomly divided into four groups (5 mice/group): control group (DMSO+PBS), CDDP treatment group (2 mg/kg), DSF treatment group (50 mg/kg), and CDDP-DSF combination treatment group. All groups were supplemented with copper ions (3 mg/kg Copper (II) Gluconate) when the mice were treated. The drug was given by intraperitoneal injection every 3 days for 5 weeks. The tumor size was measured using a caliper every 3 days for 5 weeks, and then calculated by a formula: Volume = (length × width × width)/2. At the end of the experiment, the mice were

euthanized by CO_2 asphyxiation. The tumors were dissected, weighted, and then fixed in 4% paraformaldehyde for 24 hr. H&E and immunohistochemistry staining were performed as previously described [23].

Synergistic assessment of drug combination

The combination index (CI) method of Chou and Talalay was used to quantitatively assess drug synergy [24]. When a CI value is less than 1, the drug combination indicates synergy.

Statistical analysis

Experimental data were analyzed using PRISM5 software (GraphPad Software Inc., USA) and R software (v4.3.1). For in vitro experiments, data are presented as mean ± standard deviation. Comparisons among multiple groups were performed using one-way ANOVA followed by Newman-Keuls post hoc tests, while comparisons between two groups used two-tailed Student's t-tests. Dynamic changes in tumor volume (with time variables) were analyzed by two-way repeated measures ANOVA to assess main effects of time, treatment, and their interaction effects. If the interaction effect was significant ($P<0.05$), post hoc multiple comparisons were adjusted using the Bonferroni method. Endpoint tumor weights were compared via one-way ANOVA, and survival analysis was conducted using the log-rank test (via the "survival" package in R, with optimal cutoff values determined by the maxstat algorithm; hazard ratios [HR] and 95% confidence intervals were calculated using the Cox proportional hazards model). Drug synergy was quantified by the Chou-Talalay method (Combination Index, CI<1 indicates synergy). RNA-seq differential genes were filtered using thresholds of |log2 (Fold Change)| >1 and FDR<0.05 (Benjamini-Hochberg correction). Significance levels were defined as $P<0.05$.

Result

High-throughput drug screening found that DSF enhanced the sensitivity of SCLC cells to CDDP

In order to find a drug that can increase the sensitivity of SCLC to CDDP, we used a high-throughput screening approach. 1092 FDA-approved drugs were screened when combined with CDDP treatment in SCLC cells. We found that DSF at low dose increased the inhibitory activity of CDDP on the growth of SCLC cells (**Figure 1A**). Therefore, we further studied the combination effect of DSF and CDDP in various SCLC cell lines (H69, H82, H446 and H526) (**Figure 1B**). In order to select suitable combination doses, we first examined IC_{50} values of CDDP and DSF in SCLC cells (Supplementary Figure 1). Cell viability assay indicated that the combination of DSF and CDDP induced more cellular death in various SCLC cell lines, when compared with DSF and CDDP treatment alone. To indicate the synergistic effect of DSF and CDDP, we calculated the synergistic index in H69 and H196 cells. As indicated in **Tables 1** and **2**, the combination of DSF and CDDP showed synergistic anti-tumor effect as the values of CI in both H69 and H196 cells were less than one. Since previous studies have shown that the killing effect of DSF on cancer cells depends on copper ions, we supplemented copper ions (1 μM Copper (II) Gluconate) in cell culture medium. The results demonstrated that the synergistic activity of DSF and CDDP was enhanced when copper ions were supplemented in culture medium of SCLC cells, compared with culture medium without copper ions supplement (**Figure 1C**). These results indicate that DSF synergistically enhances anti-tumor activity of CDDP in SCLC, dependent on copper ions.

DSF enhanced CDDP-induced apoptosis in SCLC

Since CDDP induced apoptosis, we next examined the effect of the combined treatment of CDDP and DSF on apoptosis. As shown in **Figure 2A**, flow cytometry analysis indicated that CDDP and DSF combination induced more cellular apoptosis (Annexin V positive cells in Q2 and Q3) in SCLC H69 and H446 cells, compared with CDDP and DSF treatment alone. Furthermore, western blot indicated that co-treatment of CDDP and DSF induced more PARP cleavage (apoptotic marker) in SCLC (**Figure 2B**). These results indicate that DSF enhances CDDP-induced cellular apoptosis in SCLC.

The potential targets of combination treatment of DSF and CDDP in SCLC

In order to further explore the mechanism contributing to the synergistic anti-tumor effect of

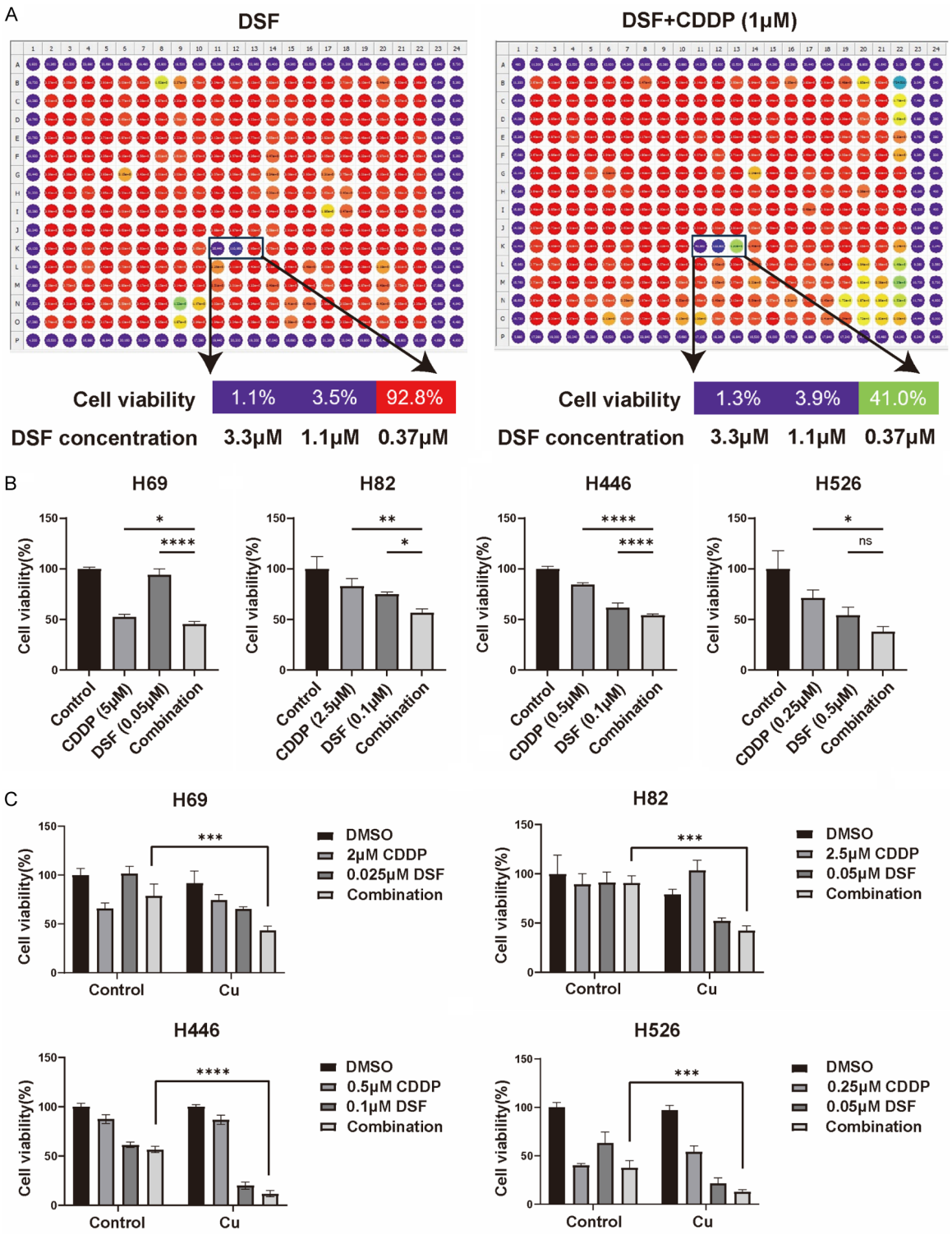

Figure 1. High-throughput drug screening identifies DSF that can enhance the sensitivity of SCLC to CDDP. A. The plate map of high-throughput drug screen that identified DSF, which can enhance the anti-proliferative activity of CDDP in SCLC H196 cells. The growth inhibition of H196 cells by DSF alone or combined with 1 μM CDDP was indicated. B. DSF significantly increased CDDP-induced growth inhibition in SCLC cells. The SCLC cells (H69, H82, H446 and H526 cells) were treated with DMSO control, DSF, CDDP or the combination of DSF and CDDP for 72 hr. After treatment, cell viability was detected by CellTiter-Glo Luminescent assay. C. The supplement of copper ions increases the synergistic activity of CDDP and DSF in SCLC. The SCLC cells (H69, H82, H446 and H526 cells) were treated with DMSO control, DSF, CDDP or the combination of DSF and CDDP for 72 hr. Copper (II) Gluconate (1 μM) was supplemented in the Cu group. After treatment, cell viability was detected by CellTiter-Glo Luminescent assay.

Table 1. Combination index (CI) of disulfiram and cisplatin in H69 cells

Disulfiram dose (nM) D1	Cisplatin dose (nM) D2	Mean growth inhibition (%) x	Dose of Disulfiram alone with same inhibition (nM) Dx1	Dose of Cisplatin alone with same inhibition (nM) Dx2	CI
100	500	86.4	244	102589	0.41
100	1000	87.7	240	109370	0.43
100	2500	85.9	218	87902	0.49
200	500	96.5	263	239883	0.76
200	1000	96.4	271	239221	0.74
200	2000	95.6	251	187254	0.81
200	2500	96.1	271	221615	0.74
200	5000	95.1	251	173340	0.82

Table 2. Combination index (CI) of disulfiram and cisplatin in H196 cells

Disulfiram dose (nM) D1	Cisplatin dose (nM) D2	Mean growth inhibition (%) x	Dose of Disulfiram alone with same inhibition (nM) Dx1	Dose of Cisplatin alone with same inhibition (nM) Dx2	CI
100	10000	92	3286	45248	0.25
100	5000	90	1707	36872	0.19
100	500	82	189	25445	0.54

DSF and CDDP co-treatment in SCLC, we performed RNA-seq analysis of H69 cells treated by DMSO control, 0.025 μM DSF, 2 μM CDDP and combination treatment. All detected RNAs were showed in the heatmap (**Figure 3A**). Firstly, we analyzed the differentially expressed genes (CDDP vs DMSO, LogFC>1 and FDR< 0.05). We identified 94 up-regulated and 59 down-regulated genes by CDDP treatment, compared to DMSO control treatment. The expression changes of these genes may cause the resistance of SCLC cells to CDDP (**Figure 3B**). Secondly, we analyzed the differentially expressed genes (Combination vs CDDP, LogFC>1 and FDR<0.05). We identified 72 up-regulated and 146 down-regulated genes by combination treatment, compared to CDDP treatment (**Figure 3B**). Finally, the Venn diagrams showed the intersections of the differentially expressed genes (up-regulation and down-regulation) in the two comparisons. The results indicated that 30 genes were significantly up-regulated in the CDDP group compared with DMSO group, while these genes were significantly down-regulated in the combination treatment compared with CDDP treatment. 14 genes were significantly down-regulated in the CDDP group compared with DMSO group, while these genes were significantly up-regulated in the combination treatment compared with CDDP treatment (**Figure 3B**). The 44 genes may be targets of DSF to reverse CDDP resistance in SCLC. Subsequently, we screened the 44 genes by KM survival analysis using GSE60052 dataset. Seven genes were identified to be significantly associated with the survival of SCLC patients, including CBS, CHKB.CPT1B, PCDHA1, GNB3, ICAM3, CEP170P1 and ZNF157 (**Figure 3C** and Supplementary Figure 2). Previous studies have demonstrated that cystathione-beta synthase (CBS) promoted tumor progression and therapeutic resistance [25]. DSF-Cu complex effectively inhibited the enzymatic activity of CBS [26]. Based on these previous studies, we hypothesized that CBS was the target of DSF synergized with CDDP in killing SCLC cells. Furthermore, we validated that CBS expression was elevated by different doses of CDDP treatment in H69 and H446 cells (**Figure 3D**). The elevation of CBS expression was down-regulated by the co-treatment of DSF and CDDP in H69 and H446 cells (**Figure 3E**). These results suggest that CBS is a potential target of combination treatment of DSF and CDDP in SCLC.

The down-regulation of CBS increased the sensitivity of SCLC cells to CDDP

Next, to indicate whether CBS affects the sensitivity SCLC cells to CDDP, we knocked-down

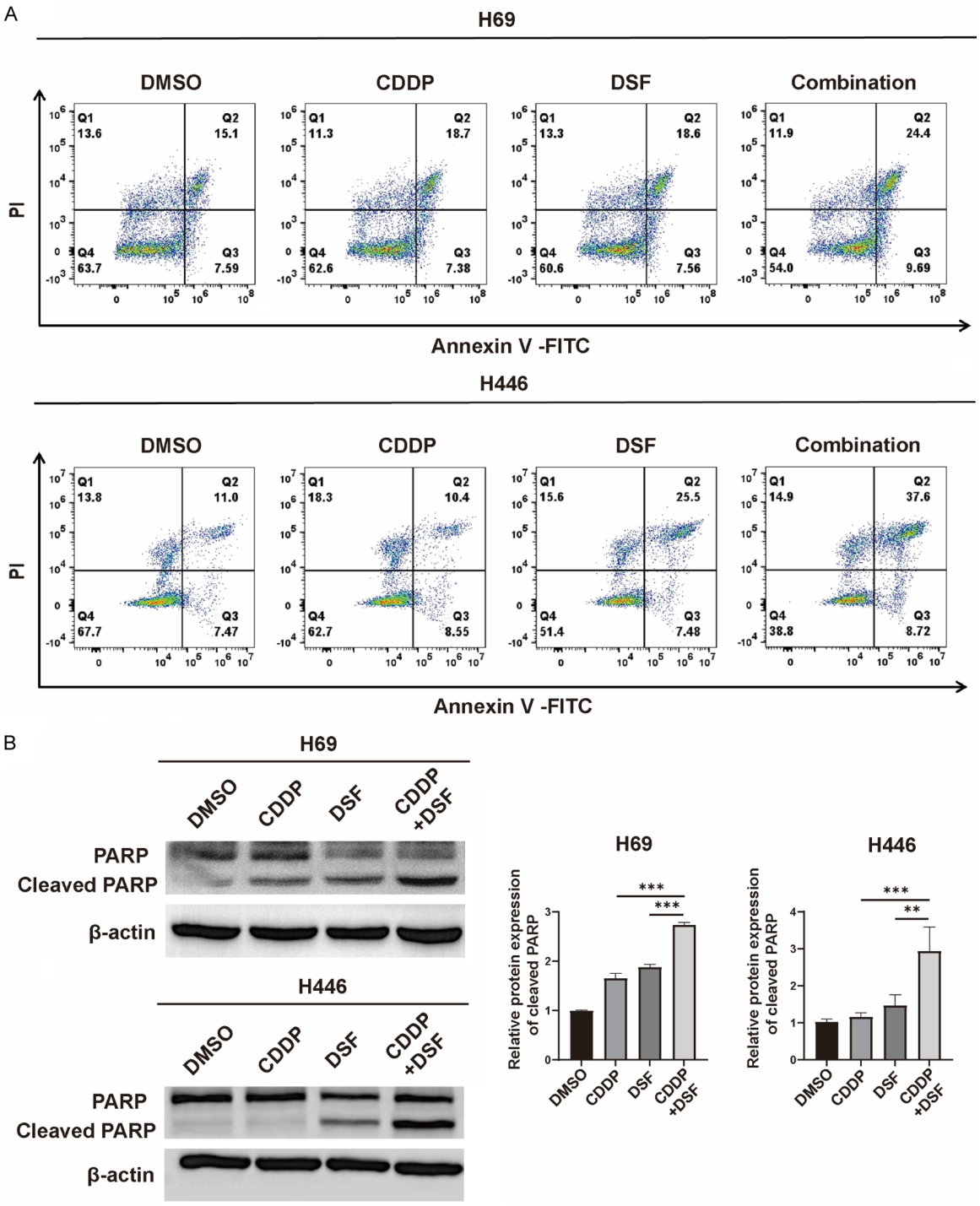

Figure 2. DSF promotes CDDP-induced apoptosis in SCLC. A. DSF enhanced CDDP-induced cellular apoptosis in SCLC cells. H69 cells were treated with DMSO control, CDDP (2 μM), DSF (0.025 μM), and the DSF-CDDP combination for 24 hr. H446 cells were treated with DMSO control, CDDP (0.5 μM), DSF (0.1 μM), and the DSF-CDDP combination for 12 hr. Copper (II) Gluconate (1 μM) was supplemented in the all treatment. After treatment, cell apoptosis was detected by Annexin V apoptotic assay. B. DSF and CDDP co-treatment induced stronger apoptosis as indicated by PARP cleavage. H69 cells were treated with DMSO control, CDDP (2 μM), DSF (0.025 μM), and the DSF-CDDP combination for 24 hr. H446 cells were treated with DMSO control, CDDP (0.5 μM), DSF (0.1 μM), and the DSF-CDDP combination for 12 hr. Copper (II) Gluconate (1 μM) was supplemented in the all treatment. PARP and cleaved PARP were detected by western blot. β-Actin was used as loading control. Intensity of cleaved PARP band was quantified by ImageJ, and then normalized by the expression of β-Actin.

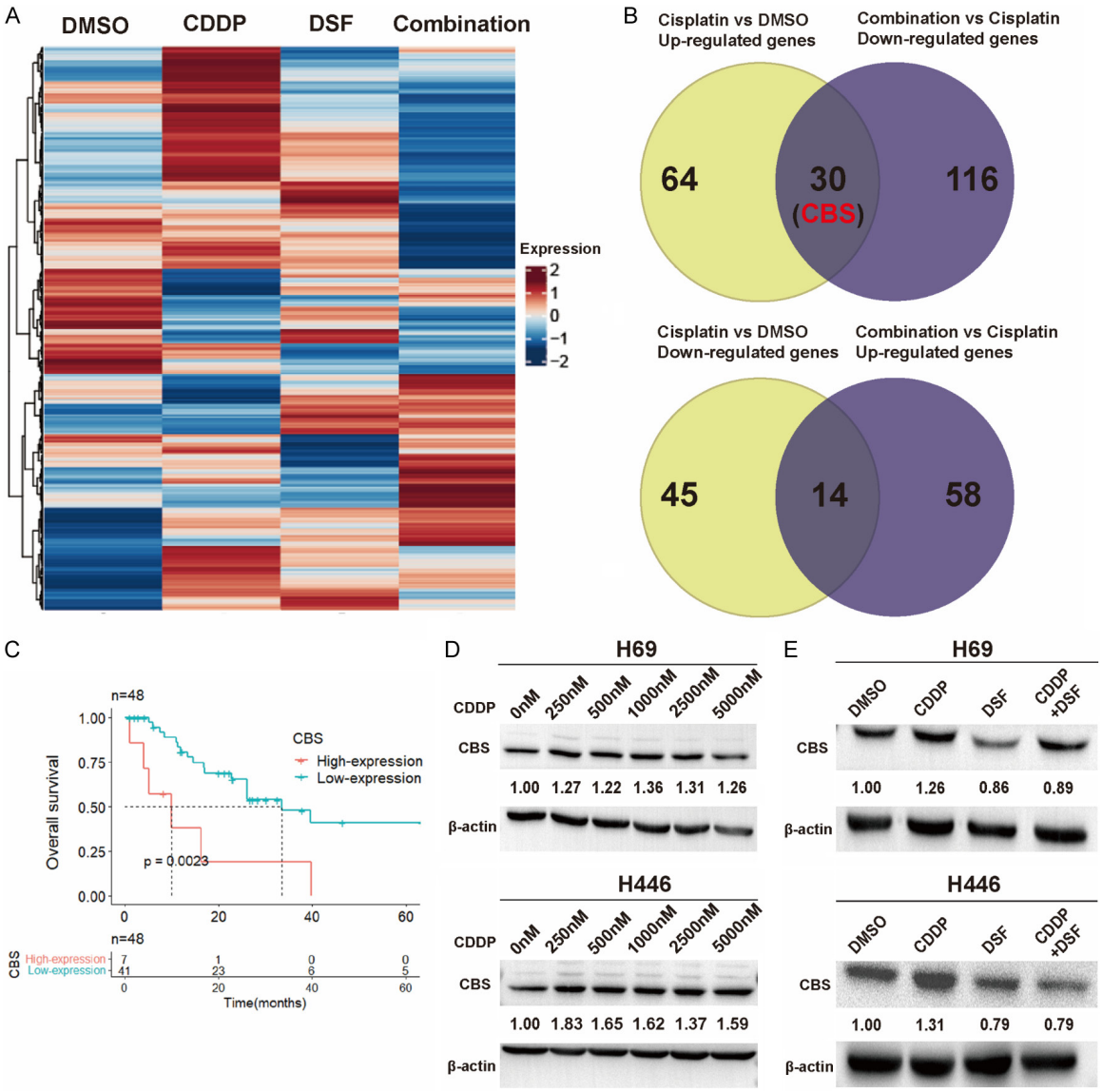

Figure 3. RNA-seq identifies the potential target of DSF and CDDP combination. A. The heatmap of all RNAs detected in H69 cells after treatments. H69 cells were treated by DMSO control, CDDP (2 μM), DSF (0.025 μM), and the combination treatment of CDDP (2 μM) and DSF (0.025 μM) for 24 hr. Copper (II) Gluconate (1 μM) was supplemented in the all treatment. B. Venn diagrams show the intersections of the differentially expressed mRNA among the two comparisons. C. KM curve shows the association of CBS expression with overall survival in 48 SCLC patients from the GSE60052 dataset. D. Western blot shows that CDDP induces the expression of CBS in H69 cells and H446 cells. β-actin was used as loading control. E. Western blot shows that CDDP and DSF co-treatment decreases CBS expression induced by CDDP in H69 and H446 cells. β-actin was used as loading control.

CBS by transfecting CBS siRNA in SCLC cells (**Figure 4A**). Western blot indicated that CDDP induced more cleaved PARP (apoptotic marker), when CBS was knocked-down in H446 cells (**Figure 4B**). Flow cytometry assay demonstrated that CDDP induced more Annexin V positive cells (apoptotic marker), when CBS was knocked-down in H446 cells (**Figure 4C**). These results indicate that CBS is involved in the regulation of SCLC cells to CDDP sensitivity.

CDDP treatment increased H_2S level, which was reduced by the combination treatment of DSF and CDDP

CBS is a critical enzyme in the transsulfur pathway and can produce H_2S [27]. Firstly, we examined the production of H_2S after the treatment in H446 cells. The data indicated that CDDP increased the level of H_2S, while the combination treatment of DSF and CDDP inhibited

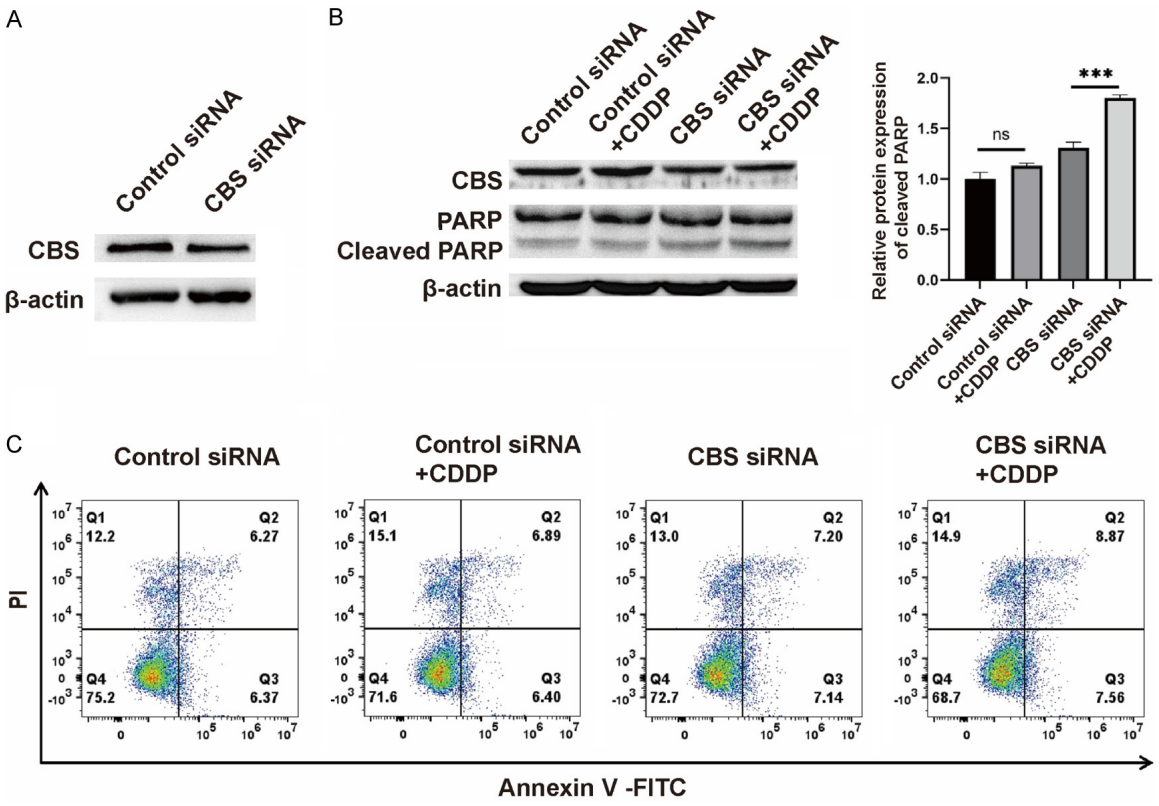

Figure 4. The down-regulation of CBS increases CDDP-induced cell apoptosis in SCLC. A. Western blot indicates that CBS is knocked down in H446 cells. B. Western blot indicates that PARP cleavage is increased in H446 cells with CBS knock-down. H446 cells were transiently transfected with CBS and control siRNA for 24 hr, and then transfected cells were treated with DMSO and CDDP (1 μM) for 24 hr. Intensity of cleaved PARP band was quantified by ImageJ, and then normalized by the expression of β-Actin. C. Flow cytometry indicates that CBS knock-down increases the apoptosis of H446 cells induced by CDDP treatment. H446 cells were transiently transfected with CBS and control siRNA for 24 hr, and then transfected cells were treated with DMSO and CDDP (1 μM) for 24 hr.

CDDP-induced H_2S production in H446 cells (**Figure 5A**). CDDP is able to induce apoptosis through the generation of ROS. H_2S is a reducing agent that can scavenge ROS. Therefore, we hypothesized that CDDP-induced H_2S reduced ROS level, which could lead to the insensitivity of cancer cells to CDDP treatment. Indeed, when H_2S level was reduced by the co-treatment of DSF and CDDP, ROS level was elevated in H446 cells (**Figure 5B**). In order to indicate that the combination of CDDP and DSF induce apoptosis of SCLC cells via the inhibition of H_2S, we conducted H_2S rescue experiment. H446 cells were cultured in the medium with 10 μM NaSH to supplement H_2S. As shown in **Figure 5C**, the elevation of H_2S level significantly reduced the growth inhibition of H446 cells by CDDP and DSF co-treatment. These results indicate that DSF sensitizes SCLC cells to CDDP via the inhibition of H_2S.

Combination of DSF and CDDP exhibited significant anti-tumor activity in vivo

Next, we determined the *in vivo* antitumor efficacy of DSF and CDDP combination in an SCLC model. Mice were subcutaneously inoculated with H69 SCLC cells. When the tumor size reached 4-5 mm in diameter, the mice were randomized into four groups for vehicle control, CDDP (2 mg/kg), DSF (50 mg/kg), and combination treatment. Treatments were given every 3 days for 33 days, and all treatments were supplemented with copper ions (3 mg/kg Copper (II) Gluconate). As shown in **Figure 6A**, CDDP single agent resulted in the growth inhibition. However, the addition of DSF significantly reduced the tumor size, compared with CDDP treatment alone. At the end of the experiment, we dissected the tumors from the mice. We found that tumors' weight from the combined treatment group was significantly reduced,

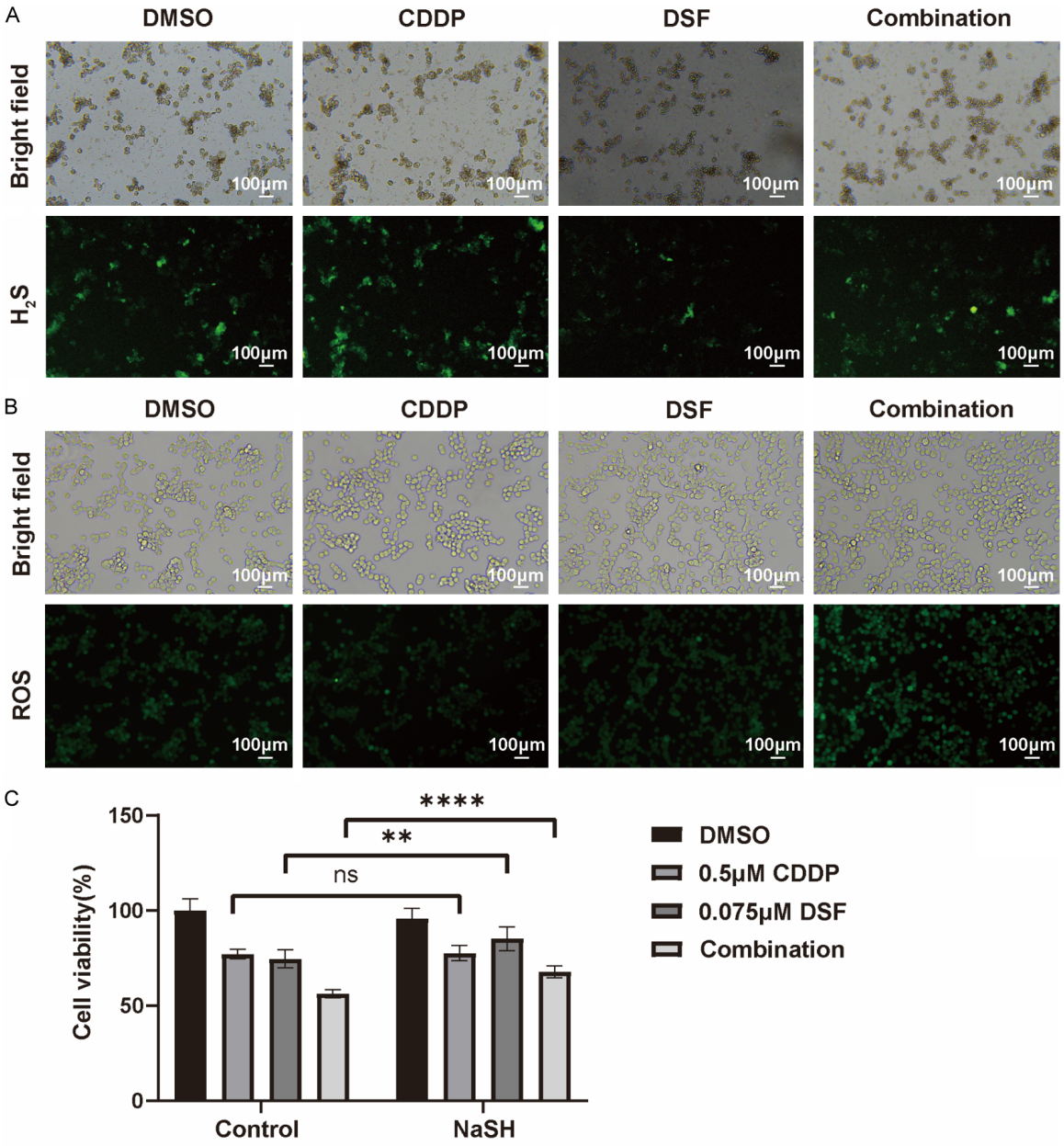

Figure 5. Combination of DSF and CDDP decreases the level of H_2S, and increases ROS. A. The combination of DSF and CDDP inhibits intracellular H_2S generation. H446 cells were treated with DMSO control, CDDP (0.5 μM), DSF (0.1 μM), or the combination of CDDP and DSF for 4 hr. After treatment, cells were stained with WSP-5, and then H_2S (green fluorescence) was detected by fluorescence microscopy. B. The combination of DSF and CDDP induces more intracellular ROS generation. H446 cells were treated with DMSO control, CDDP (0.5 μM), DSF (0.1 μM), or the combination of CDDP and DSF for 4 hr. After treatment, cells were stained with DCFH-DA, and then ROS (green fluorescence) was detected by fluorescence microscopy. C. The elevation of H_2S reverses the growth inhibition induced by the combined treatment of DSF and CDDP in H446 cells. NaSH (10 μM) was added to culture medium to produce H_2S. In the culture medium with or without NaSH (10 μM), H446 cells were treated with DMSO control, CDDP, DSF, or the combination CDDP and DSF for 72 hr. After treatment, growth inhibition was determined by CellTiterGlo Luminescent assay.

compared with CDDP treatment alone (**Figure 6B** and **6C**). The combination treatments did not appear to affect the weights of the mice, indicating minimal toxicity of these combinations *in vivo* (**Figure 6D**). Furthermore, by immunohistochemical staining, the tumors of the combination group displayed a remarkable reduction in Ki-67 proliferation marker staining

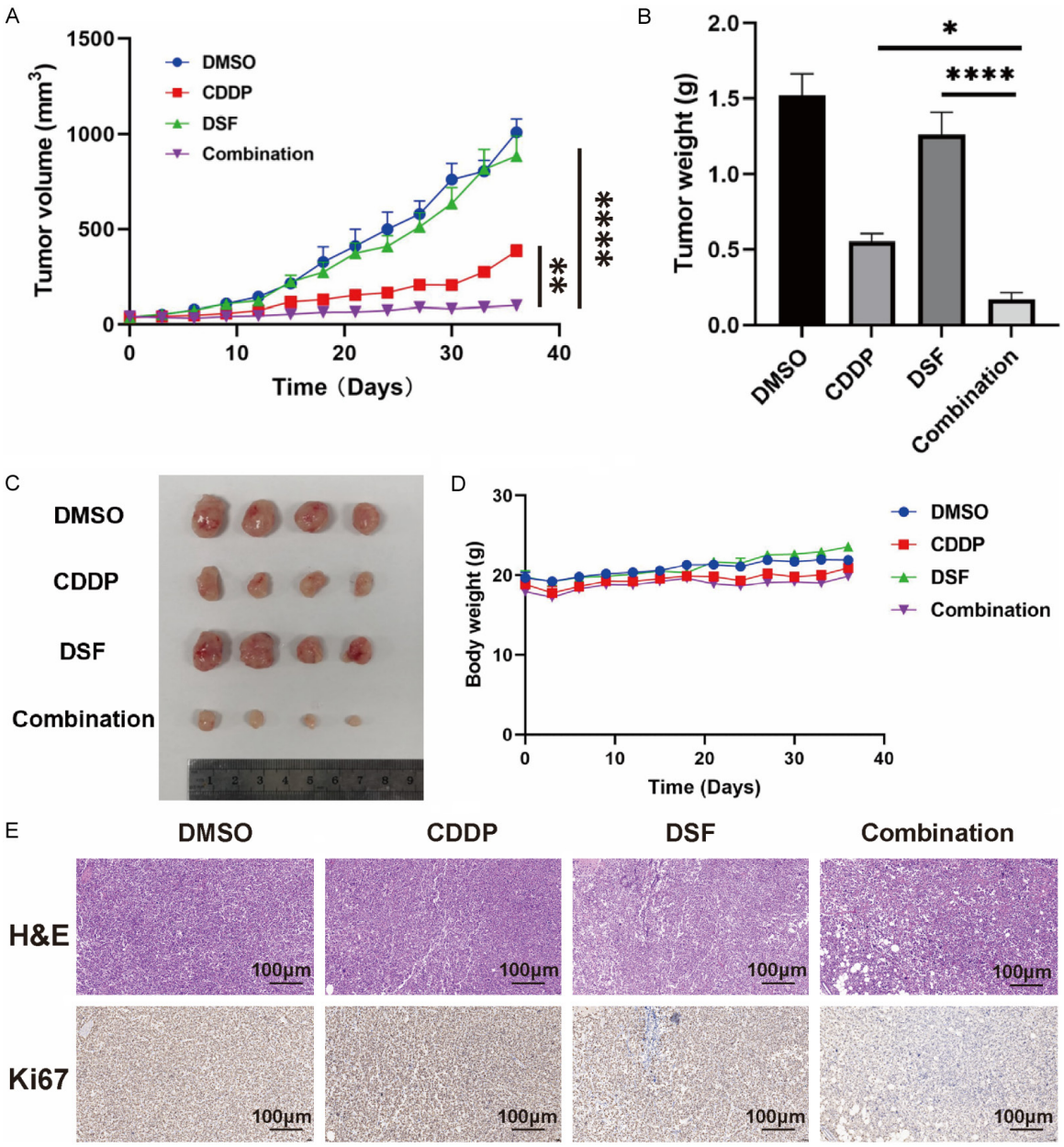

Figure 6. Combination of DSF and CDDP inhibits SCLC tumor growth *in vivo*. A. The combination of DSF and CDDP remarkably suppresses tumor growth in mouse model with SCLC H69 xenografts. Mice with H69 xenografts were treated by DMSO control, 50 mg/kg DSF, 2 mg/kg CDDP, or the combination of DSF and CDDP every three days for 5 weeks. All treatments were supplemented with Copper (II) Gluconate (3 mg/kg). The mean tumor size ± SEM is shown. B. At the end of the experiment, tumor weight in combination group was significantly decreased compared to CDDP group. The mean tumor weight ± SEM is shown. C. Imaging of tumors from each group. The tumors were excised at the end of the experiment. D. Body weights of the nude mice during treatment. E. H&E staining and immunohistochemistry detection of Ki67.

compared with single agent treatment alone, demonstrating that the combination could markedly halt SCLC tumor cell proliferation *in vivo* (**Figure 6E**). These results indicate that DSF is able to enhance anti-tumor activity of CDDP in SCLC *in vivo*.

Discussion

Chemotherapy resistance is a major issue for SCLC treatment in the clinic. In this study, we screened FDA-approved drugs to seek a drug which can enhance the sensitivity of SCLC to

CDDP. We found that DSF was able to increase the anti-tumor activity of CDDP in SCLC, dependent on copper ions. We found that CDDP induced the CBS expression, and the addition of DSF decreased CDDP-induced CBS expression. Furthermore, the co-treatment of DSF and CDDP reduced the production of H_2S, and whereas increased the level of ROS. The study suggests that CBS is a potential target of the combination treatment of DSF and CDDP in SCLC.

CBS catalyzes homocysteine to produce H_2S [25]. Recent studies have demonstrated that CBS plays an important role in cancer development and therapeutic resistance. Bhattacharyya et al. indicated that the silence of CBS decreased level of GSH and H_2S production, thereby promoting an increase of ROS and CDDP-induced apoptosis in ovarian cancer [28]. High levels of CBS and endogenous H_2S were detected in tumor tissues in NSCLC, and H_2S promotes tumor angiogenesis by stimulating the expression of VEGF through HIF-1α [29]. CBS was highly expressed in esophageal squamous cell carcinoma, and CBS/H_2S promoted lymph node metastasis by activating SIRT1 signaling pathway [30]. In colon cancer, H_2S produced by CBS was able to maintain biological energy of cancer cells and promote tumor growth and angiogenesis [31]. At the same time, it has been indicated that the inhibition of CBS expression could reverse 5-Fu resistance in colon cancer [32]. It has been reported that CBS was highly expressed in breast cancer, and the high CBS expression was associated with the progression of breast cancer [33]. Cysteine in tumors was limited, so CBS-mediated cysteine synthesis was critical for tumor growth [34]. In Triple-negative breast cancer, HIF-1-induced CBS upregulation provided an alternative source of cysteine for glutathione synthesis and protects cells from Ferroptosis [35]. In prostate cancer, HSF1 regulated the conversion of homocysteine to cystathionine in the transsulfuration pathway by inducing CBS. CBS knock-down reduced the growth of prostate cancer cells and induced tumor cell death [36]. Our study found that CDDP induced CBS expression and H_2S elevation in SCLC, which could promote CDDP resistance. However, the co-treatment of DSF and CDDP reduced CBS and H_2S. Therefore, our study suggests that CBS is a potential target of the combination treatment of DSF and CDDP in SCLC.

H_2S has a wide range of effects on tumor growth, such as cell proliferation, energy production, apoptotic signaling, angiogenesis and so on. It has been reported that low doses of H_2S could promote the phosphorylation of AKT and stimulate the growth of liver cancer cells [37]. H_2S sulfhydrated MEK, which interacted with PARP-1, thus promoting DNA damage repair [38]. In addition, H_2S facilitated the repair of mitochondrial DNA and promoted mitochondrial function in cancer cells [39]. Endogenous H_2S could also promote the sulfhydrylation of p65 and increase the transcriptional activity of p65, thereby enhancing the expression of anti-apoptotic proteins [40]. H_2S regulated the redox state of thioredoxin (Trx) and inhibited the redox damage of cells [41]. Wahafu et al. indicated that H_2S contributed to CDDP resistance in urothelial cell carcinoma of the bladder [42]. Depletion of endogenous H_2S production significantly inhibited the growth of nasopharyngeal carcinoma through ROS/MAPK pathway [43]. H_2S level also affected tumor immune microenvironment. Yue et al. have demonstrated that reducing H_2S levels increased the $CD8^+$ T-cell/Treg ratio in tissues of colorectal cancer [44]. Our study showed that CDDP treatment increased the level of H_2S, which may reduce ROS level, thereby promoting CDDP resistance. The combination treatment of CDDP and DSF decreased the level of H_2S, and increased the level of ROS. Therefore, our study suggests that H_2S is a mediator of CDDP resistance in SCLC.

Our study showed that DSF synergistically enhances anti-tumor activity of CDDP in SCLC. CBS/H_2S is the targets of DSF and CDDP co-treatment in SCLC. Our study provides a rational basis for further clinical study to re-purpose DSF as a sensitizer of cisplatin-based therapy in SCLC patients.

Acknowledgements

This work was supported by the National Natural Science Foundation of China (Grant Number: 81872438), the Collaborative Innovation Program of Hefei Science Center, CAS (Grant Number: 2022HSC-CIP015), and the Program of Clinical Medical Translational Research in Anhui Province (Grant Number: 202304295107020092).

Disclosure of conflict of interest

None.

Abbreviations

NSCLC, Non-small cell lung cancer; SCLC, Small cell lung cancer; CDDP, Cisplatin; DSF, Disulfiram; DTC, Diethyldithiocarbamate; CBS, Cystathionine β-synthase; CTAB, Hexadecyltrimethylammonium bromide; CI, Combination index.

Address correspondence to: Drs. Bo Hong and Hongzhi Wang, Hefei Cancer Hospital of CAS, Institute of Health and Medical Technology, Hefei Institutes of Physical Science, Chinese Academy of Sciences (CAS), No. 350 Shushanhu Road, Hefei 230031, Anhui, China. E-mail: bhong@hmfl.ac.cn (BH); wanghz@hfcas.ac.cn (HZW)

References

[1] Lahiri A, Maji A, Potdar PD, Singh N, Parikh P, Bisht B, Mukherjee A and Paul MK. Lung cancer immunotherapy: progress, pitfalls, and promises. Mol Cancer 2023; 22: 40.

[2] Liu Q, Zhang J, Guo C, Wang M, Wang C, Yan Y, Sun L, Wang D, Zhang L, Yu H, Hou L, Wu C, Zhu Y, Jiang G, Zhu H, Zhou Y, Fang S, Zhang T, Hu L, Li J, Liu Y, Zhang H, Zhang B, Ding L, Robles AI, Rodriguez H, Gao D, Ji H, Zhou H and Zhang P. Proteogenomic characterization of small cell lung cancer identifies biological insights and subtype-specific therapeutic strategies. Cell 2024; 187: 184-203, e128.

[3] Rudin CM, Brambilla E, Faivre-Finn C and Sage J. Small-cell lung cancer. Nat Rev Dis Primers 2021; 7: 3.

[4] George J, Lim JS, Jang SJ, Cun Y, Ozretić L, Kong G, Leenders F, Lu X, Fernández-Cuesta L, Bosco G, Müller C, Dahmen I, Jahchan NS, Park KS, Yang D, Karnezis AN, Vaka D, Torres A, Wang MS, Korbel JO, Menon R, Chun SM, Kim D, Wilkerson M, Hayes N, Engelmann D, Pützer B, Bos M, Michels S, Vlasic I, Seidel D, Pinther B, Schaub P, Becker C, Altmüller J, Yokota J, Kohno T, Iwakawa R, Tsuta K, Noguchi M, Muley T, Hoffmann H, Schnabel PA, Petersen I, Chen Y, Soltermann A, Tischler V, Choi CM, Kim YH, Massion PP, Zou Y, Jovanovic D, Kontic M, Wright GM, Russell PA, Solomon B, Koch I, Lindner M, Muscarella LA, la Torre A, Field JK, Jakopovic M, Knezevic J, Castaños-Vélez E, Roz L, Pastorino U, Brustugun OT, Lund-Iversen M, Thunnissen E, Köhler J, Schuler M, Botling J, Sandelin M, Sanchez-Cespedes M, Salvesen HB, Achter V, Lang U, Bogus M, Schneider PM, Zander T, Ansén S, Hallek M, Wolf J, Vingron M, Yatabe Y, Travis WD, Nürnberg P, Reinhardt C, Perner S, Heukamp L, Büttner R, Haas SA, Brambilla E, Peifer M, Sage J and Thomas RK. Comprehensive genomic profiles of small cell lung cancer. Nature 2015; 524: 47-53.

[5] George J, Maas L, Abedpour N, Cartolano M, Kaiser L, Fischer RN, Scheel AH, Weber JP, Hellmich M, Bosco G, Volz C, Mueller C, Dahmen I, John F, Alves CP, Werr L, Panse JP, Kirschner M, Engel-Riedel W, Jürgens J, Stoelben E, Brockmann M, Grau S, Sebastian M, Stratmann JA, Kern J, Hummel HD, Hegedüs B, Schuler M, Plönes T, Aigner C, Elter T, Toepelt K, Ko YD, Kurz S, Grohé C, Serke M, Höpker K, Hagmeyer L, Doerr F, Hekmath K, Strapatsas J, Kambartel KO, Chakupurakal G, Busch A, Bauernfeind FG, Griesinger F, Luers A, Dirks W, Wiewrodt R, Luecke A, Rodermann E, Diel A, Hagen V, Severin K, Ullrich RT, Reinhardt HC, Quaas A, Bogus M, Courts C, Nürnberg P, Becker K, Achter V, Büttner R, Wolf J, Peifer M and Thomas RK. Evolutionary trajectories of small cell lung cancer under therapy. Nature 2024; 627: 880-889.

[6] Oronsky B, Abrouk N, Caroen S, Lybeck M, Guo X, Wang X, Yu Z and Reid T. A 2022 update on extensive stage Small-Cell Lung Cancer (SCLC). J Cancer 2022; 13: 2945-2953.

[7] Liu X, Wang W, Yin Y, Li M, Li H, Xiang H, Xu A, Mei X, Hong B and Lin W. A high-throughput drug screen identifies auranofin as a potential sensitizer of cisplatin in small cell lung cancer. Invest New Drugs 2019; 37: 1166-1176.

[8] Zeng M, Wu B, Wei W, Jiang Z, Li P, Quan Y and Hu X. Disulfiram: a novel repurposed drug for cancer therapy. Chin Med J (Engl) 2024; 137: 1389-1398.

[9] Yang Z, Guo F, Albers AE, Sehouli J and Kaufmann AM. Disulfiram modulates ROS accumulation and overcomes synergistically cisplatin resistance in breast cancer cell lines. Biomed Pharmacother 2019; 113: 108727.

[10] Wang W, McLeod HL and Cassidy J. Disulfiram-mediated inhibition of NF-kappaB activity enhances cytotoxicity of 5-fluorouracil in human colorectal cancer cell lines. Int J Cancer 2003; 104: 504-511.

[11] Xu Y, Lu L, Luo J, Wang L, Zhang Q, Cao J and Jiao Y. Disulfiram alone functions as a radiosensitizer for pancreatic cancer both in vitro and in vivo. Front Oncol 2021; 11: 683695.

[12] Zeng C, Nie D, Wang X, Zhong S, Zeng X, Liu X, Qiu K, Peng X, Zhang W, Chen S, Zha X, Chen C, Chen Z, Wang W and Li Y. Combined targeting of GPX4 and BCR-ABL tyrosine kinase selectively compromises BCR-ABL+ leukemia stem cells. Mol Cancer 2024; 23: 240.

[13] Zheng X, Liu Z, Mi M, Wen Q, Wu G and Zhang L. Disulfiram improves the anti-PD-1 therapy efficacy by regulating PD-L1 expression via epigenetically reactivation of IRF7 in triple negative breast cancer. Front Oncol 2021; 11: 734853.
[14] Yang L, Sui H, Ding Y, Zhu Y, Song X, Zhang Y, Fan G, Wang J, Cui X, Jiang Y, Zhao S, Hong Y, Mu N, Tian Z, Zhao Y, Li P and Zhao X. Disulfiram impairs USP21-mediated MOF-K257 deubiquitination to inhibit esophageal squamous cell carcinoma progression. Cancer Lett 2024; 611: 217419.
[15] Wang Q, Zhu T, Miao N, Qu Y, Wang Z, Chao Y, Wang J, Wu W, Xu X, Xu C, Xia L and Wang F. Disulfiram bolsters T-cell anti-tumor immunity through direct activation of LCK-mediated TCR signaling. EMBO J 2022; 41: e110636.
[16] Terashima Y, Toda E, Itakura M, Otsuji M, Yoshinaga S, Okumura K, Shand FHW, Komohara Y, Takeda M, Kokubo K, Chen MC, Yokoi S, Rokutan H, Kofuku Y, Ohnishi K, Ohira M, Iizasa T, Nakano H, Okabe T, Kojima H, Shimizu A, Kanegasaki S, Zhang MR, Shimada I, Nagase H, Terasawa H and Matsushima K. Targeting FROUNT with disulfiram suppresses macrophage accumulation and its tumor-promoting properties. Nat Commun 2020; 11: 609.
[17] Chen D, Cui QC, Yang H and Dou QP. Disulfiram, a clinically used anti-alcoholism drug and copper-binding agent, induces apoptotic cell death in breast cancer cultures and xenografts via inhibition of the proteasome activity. Cancer Res 2006; 66: 10425-10433.
[18] Allensworth JL, Evans MK, Bertucci F, Aldrich AJ, Festa RA, Finetti P, Ueno NT, Safi R, McDonnell DP, Thiele DJ, Van Laere S and Devi GR. Disulfiram (DSF) acts as a copper ionophore to induce copper-dependent oxidative stress and mediate anti-tumor efficacy in inflammatory breast cancer. Mol Oncol 2015; 9: 1155-1168.
[19] Wang K, Michelakos T, Wang B, Shang Z, DeLeo AB, Duan Z, Hornicek FJ, Schwab JH and Wang X. Targeting cancer stem cells by disulfiram and copper sensitizes radioresistant chondrosarcoma to radiation. Cancer Lett 2021; 505: 37-48.
[20] Gao X, Huang H, Pan C, Mei Z, Yin S, Zhou L and Zheng S. Disulfiram/Copper induces immunogenic cell death and enhances CD47 blockade in hepatocellular carcinoma. Cancers (Basel) 2022; 14: 4715.
[21] Skrott Z, Mistrik M, Andersen KK, Friis S, Majera D, Gursky J, Ozdian T, Bartkova J, Turi Z, Moudry P, Kraus M, Michalova M, Vaclavkova J, Dzubak P, Vrobel I, Pouckova P, Sedlacek J, Miklovicova A, Kutt A, Li J, Mattova J, Driessen C, Dou QP, Olsen J, Hajduch M, Cvek B, Deshaies RJ and Bartek J. Alcohol-abuse drug disulfiram targets cancer via p97 segregase adaptor NPL4. Nature 2017; 552: 194-199.
[22] Peng B, Chen W, Liu C, Rosser EW, Pacheco A, Zhao Y, Aguilar HC and Xian M. Fluorescent probes based on nucleophilic substitution-cyclization for hydrogen sulfide detection and bioimaging. Chemistry 2014; 20: 1010-1016.
[23] Yin YP, Shi WH, Deng K, Liu XL, Li H, Lv XT, Lui VWY, Ding C, Hong B and Lin WC. Combinations of proteasome inhibitors with obatoclax are effective for small cell lung cancer. Acta Pharmacol Sin 2021; 42: 1298-1310.
[24] Ashton JC. Drug combination studies and their synergy quantification using the Chou-Talalay method--letter. Cancer Res 2015; 75: 2400.
[25] Ascenção K and Szabo C. Emerging roles of cystathionine β-synthase in various forms of cancer. Redox Biol 2022; 53: 102331.
[26] Zuhra K, Panagaki T, Randi EB, Augsburger F, Blondel M, Friocourt G, Herault Y and Szabo C. Mechanism of cystathionine-β-synthase inhibition by disulfiram: the role of bis(N,N-diethyldithiocarbamate)-copper(II). Biochem Pharmacol 2020; 182: 114267.
[27] Zuhra K, Augsburger F, Majtan T and Szabo C. Cystathionine-β-synthase: molecular regulation and pharmacological inhibition. Biomolecules 2020; 10: 697.
[28] Bhattacharyya S, Saha S, Giri K, Lanza IR, Nair KS, Jennings NB, Rodriguez-Aguayo C, Lopez-Berestein G, Basal E, Weaver AL, Visscher DW, Cliby W, Sood AK, Bhattacharya R and Mukherjee P. Cystathionine beta-synthase (CBS) contributes to advanced ovarian cancer progression and drug resistance. PLoS One 2013; 8: e79167.
[29] Wang M, Yan J, Cao X, Hua P and Li Z. Hydrogen sulfide modulates epithelial-mesenchymal transition and angiogenesis in non-small cell lung cancer via HIF-1α activation. Biochem Pharmacol 2020; 172: 113775.
[30] Liu Y, Pan L, Li Y, Deng Y, Han X, Fu H and Wang T. Cystathionine-β-synthase (CBS)/H2S system promotes lymph node metastasis of esophageal squamous cell carcinoma (ESCC) by activating SIRT1. Carcinogenesis 2022; 43: 382-392.
[31] Szabo C, Coletta C, Chao C, Módis K, Szczesny B, Papapetropoulos A and Hellmich MR. Tumor-derived hydrogen sulfide, produced by cystathionine-β-synthase, stimulates bioenergetics, cell proliferation, and angiogenesis in colon cancer. Proc Natl Acad Sci U S A 2013; 110: 12474-12479.
[32] Chen S, Yue T, Huang Z, Zhu J, Bu D, Wang X, Pan Y, Liu Y and Wang P. Inhibition of hydrogen sulfide synthesis reverses acquired resistance

to 5-FU through miR-215-5p-EREG/TYMS axis in colon cancer cells. Cancer Lett 2019; 466: 49-60.
[33] Sen S, Kawahara B, Gupta D, Tsai R, Khachatryan M, Roy-Chowdhuri S, Bose S, Yoon A, Faull K, Farias-Eisner R and Chaudhuri G. Role of cystathionine β-synthase in human breast cancer. Free Radic Biol Med 2015; 86: 228-238.
[34] Zhu J, Berisa M, Schwörer S, Qin W, Cross JR and Thompson CB. Transsulfuration activity can support cell growth upon extracellular cysteine limitation. Cell Metab 2019; 30: 865-876, e865.
[35] Wei G, Liu J, Lan J, Ji G, Xia H, Zhao Z, Yu Z, Sun R, Zhang C and Lu H. Targeting hypoxia-induced CBS expression inhibits breast cancer stem cells through the induction of ferroptosis. Genes Dis 2023; 10: 2195-2198.
[36] Hauck JS, Moon D, Jiang X, Wang ME, Zhao Y, Xu L, Quang H, Butler W, Chen M, Macias E, Gao X, He Y and Huang J. Heat shock factor 1 directly regulates transsulfuration pathway to promote prostate cancer proliferation and survival. Commun Biol 2024; 7: 9.
[37] Wu D, Li M, Tian W, Wang S, Cui L, Li H, Wang H, Ji A and Li Y. Hydrogen sulfide acts as a double-edged sword in human hepatocellular carcinoma cells through EGFR/ERK/MMP-2 and PTEN/AKT signaling pathways. Sci Rep 2017; 7: 5134.
[38] Zhao K, Ju Y, Li S, Altaany Z, Wang R and Yang G. S-sulfhydration of MEK1 leads to PARP-1 activation and DNA damage repair. EMBO Rep 2014; 15: 792-800.
[39] Szabo C. Hydrogen sulfide, an endogenous stimulator of mitochondrial function in cancer cells. Cells 2021; 10: 220.
[40] Sen N, Paul BD, Gadalla MM, Mustafa AK, Sen T, Xu R, Kim S and Snyder SH. Hydrogen sulfide-linked sulfhydration of NF-κB mediates its antiapoptotic actions. Mol Cell 2012; 45: 13-24.
[41] Mao Z, Huang Y, Zhang Z, Yang X, Zhang X, Huang Y, Sawada N, Mitsui T, Takeda M and Yao J. Pharmacological levels of hydrogen sulfide inhibit oxidative cell injury through regulating the redox state of thioredoxin. Free Radic Biol Med 2019; 134: 190-199.
[42] Wahafu W, Gai J, Song L, Ping H, Wang M, Yang F, Niu Y and Xing N. Increased H(2)S and its synthases in urothelial cell carcinoma of the bladder, and enhanced cisplatin-induced apoptosis following H(2)S inhibition in EJ cells. Oncol Lett 2018; 15: 8484-8490.
[43] Wang DY, Zhang J, Li HX, Zhang YX, Jing MR, Cai CB, Wang D, Qi HW, Wang YZ, Chen HJ, Li T, Zhai YK, Ji XY and Wu DD. Inhibition of endogenous hydrogen sulfide production suppresses the growth of nasopharyngeal carcinoma cells. Mol Carcinog 2023; 62: 652-664.
[44] Yue T, Li J, Zhu J, Zuo S, Wang X, Liu Y, Liu J, Liu X, Wang P and Chen S. Hydrogen sulfide creates a favorable immune microenvironment for colon cancer. Cancer Res 2023; 83: 595-612.

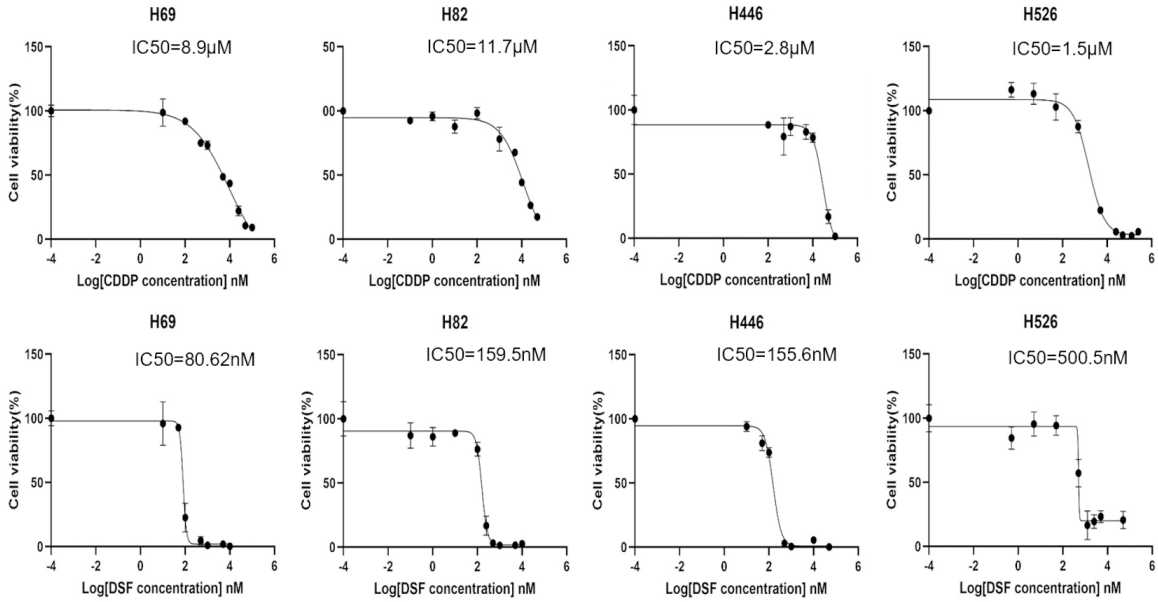

Supplementary Figure 1. The IC_{50} values of CDDP and DSF in SCLC cells (H69, H82, H446 and H526 cells).

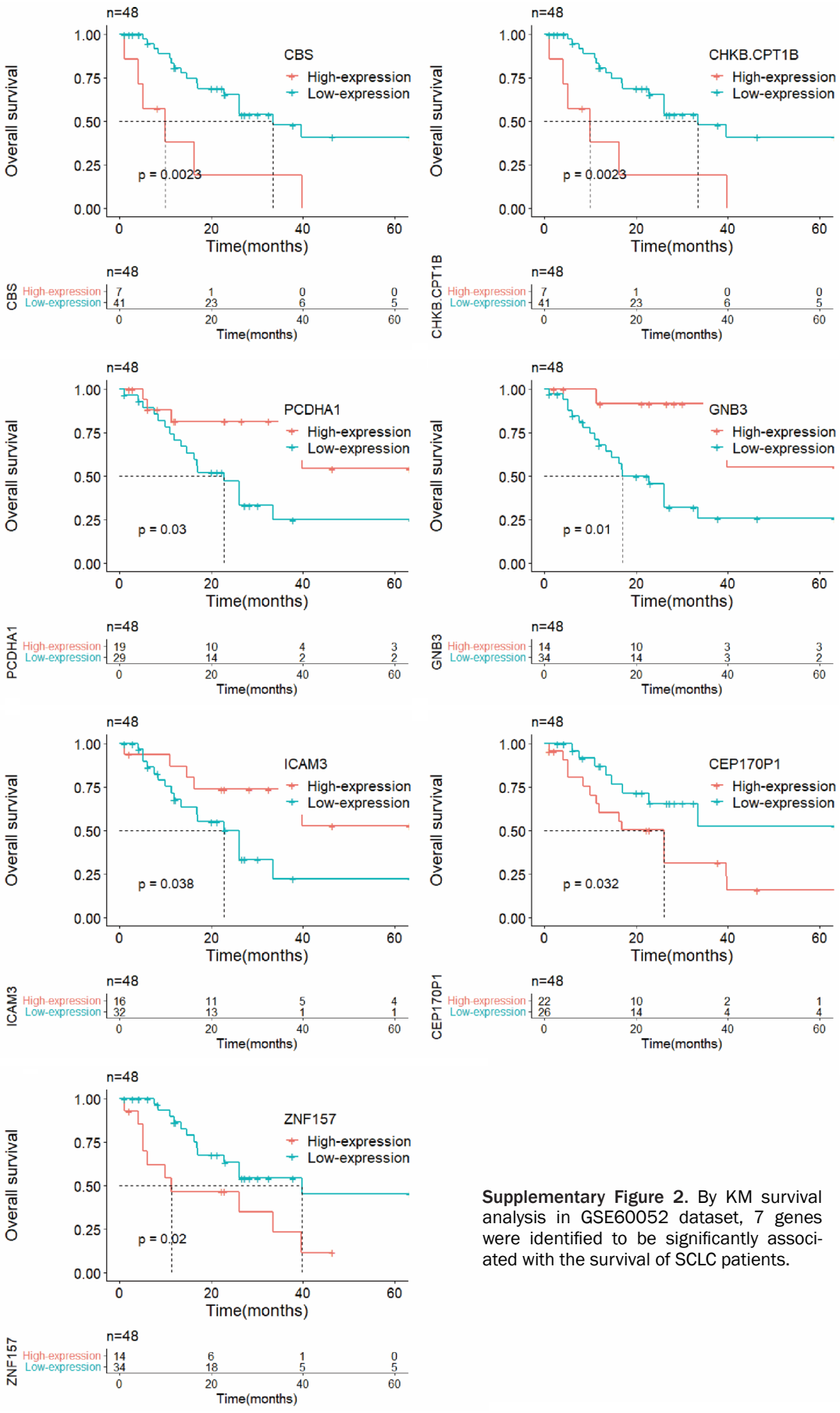

Supplementary Figure 2. By KM survival analysis in GSE60052 dataset, 7 genes were identified to be significantly associated with the survival of SCLC patients.